A CLASSICAL MODELLING OF ABANDONED MINE TAILINGS` BIOLEACHING BY AN AUTOCHTHONOUS MICROBIAL CULTURE

*Hassay Lizeth Medina-Díaz[1], Irene Acosta[1], Martín Muñoz[1], Francisco Javier López Bellido[2], José Villaseñor[1], Javier Llanos[1], Luis Rodríguez[3], Francisco Jesús Fernández-Morales[1]**

[1] Chemical Engineering Department, University of Castilla-La Mancha, ITQUIMA, Avenida Camilo José Cela s/n 13071, Ciudad Real, Spain

[2] Department of Plant Production and Agricultural Technology, School of Agricultural Engineering, University of Castilla-La Mancha, Ronda de Calatrava, s/n, 13003Ciudad Real, Spain

[3] Department of Chemical Engineering, School of Civil Engineering, University of Castilla-La Mancha, Avenida Camilo José Cela, 2, 13071 Ciudad Real, Spain

* Corresponding author: Francisco Jesús Fernández Morales

University of Castilla-La Mancha, ITQUIMA, Chemical Engineering Dept., Avda. Camilo José Cela S/N 13071, Ciudad Real, Spain.

Tel: 0034 926 295300 (ext. 6350), Fax: 0034 926 295242.

E-mail: fcojesus.fmorales@uclm.es

Orcid iD: 0000-0003-0389-6247

ABSTRACT

The aim of this study was to study and model the bioleaching of abandoned mine tailings at different pulp densities 1-20% w/v by using an autochthonous mesophilic microbial culture. Because of the importance of the ferrous-iron oxidation as sub-process on the bioleaching of sulphide mineral ores, the ferrous-iron oxidation process by the autochthonous microbial culture was studied at different ferrous-iron concentrations. A mathematical model fitted to the experimental results and the main kinetic and stoichiometric parameters were determined, being the most relevant the maximum ferrous-iron oxidation rate 5.1 (mmol Fe^{2+}/mmol C·h) and the biomass yield, 0.01 mmol C/ mmol Fe^{2+}, values very similar to that of mixed cultured dominated by *Leptospirillum* strains. This autochthonous culture was used in the bioleaching experiment carried out at different pulp densities, obtaining a maximum metal recovery in the tests carried out at 1% w/v, recovering a 90% of Cd, 60% of Zn, 30% of Cu, 25% Fe and 6% of Pb. Finally, the different leaching mechanisms were modelled by using the pyrite as ore model obtaining a bioleaching rate of 0.316 mmol Fe^{2+}/(L·h) for the direct mechanisms and a bioleaching rate for the indirect and cooperative leaching mechanisms of 0.055 Fe^{2+}/(L·h).

KEYWORDS: Modelling; rate kinetics; iron-oxidizing microorganisms; bioleaching; mine tailings

1. INTRODUCTION

The metal mining sector has been an important pole of economic development around the world. However, the accumulation of liquid and solid mining wastes after the closure of the facilities has triggered an environmental problem mainly derived from the high concentration of metals in soil as well as in underground and superficial water bodies (Azapagic, 2004). One of the most representative mining wastes are the mine tailings. The mine tailings are fine-grained minerals left-over after the extraction of the metals from the mineral ores, being its annual production about 7 billion tons (Borja et al., 2019).

Usually, the mine tailings are stockpiled around the mines without, in most of the cases, environmental treatment or control. This lack of control generates a great number of problems, mainly when the tailings are accumulated in abandoned mines, because weathering and spillage of these fine-grain minerals facilitate the dispersion of toxic metals, causing not only environmental, but also health problems (Holden, 2015).

Some of the main problems related to the mining pollution are due to its persistence and progressive accumulation in the ecosystems, (Akcil & Koldas, 2006; Ghorbani et al., 2016).

Because of the problems described, it is necessary to implement remediation technologies able to remove the pollutants and, when possible, to recover the valuable resources contained within the frame of the circular economy (Delgado et al., 2021).

An example of sustainable treatment of mining wastes is the bioleaching of sulfide minerals by means of acidophilic bacteria able to catalyze the oxidation of ferrous iron and/or reduction of sulfur compounds (He et al., 2007). These bacteria are able to produce soluble oxidized metals and sulfur as well as sulfuric acid from solid mining wastes, according to the following reactions (Eq. 1-4) (Deveci et al., 2004; Nguyen et al., 2018).

$$4\,FeSO_4 + O_2 + 2H_2SO_4 \rightarrow 2Fe_2(SO_4)_3 + 2H_2O \quad \text{[Eq. 1]}$$

$$2\,S^0 + 3\,O_2 + 2\,H_2O \rightarrow 2\,H_2SO_4 \quad \text{[Eq. 2]}$$

$$MS + 2Fe^{+3} \rightarrow M^{+2} + S^0 + 2Fe^{+2} \quad \text{[Eq. 3]}$$

$$2\,MS + O_2 + 2\,H_2SO_4 \rightarrow 2\,M^{+2} + 2\,H_2O + 2\,S^0 \quad \text{[Eq. 4]}$$

In the literature, it has been described that the bioleaching process can be carried out by three different mechanisms: direct, indirect and cooperative (Figueroa-Estrada et al., 2020; Sajjad et al., 2019). In the direct mechanisms, the bacteria catalyze the reaction through an enzymatic attack that involves physical contact between the bacteria and the mineral ore through the extracellular polymeric substances (EPS) (Huang and Li, 2014). The indirect mechanisms take place by means of chemical reactions in which the ferric ions are reduced to ferrous iron by oxidizing the metal sulfide and leaching it in its soluble form (Ciftci and Atik, 2017). The cooperative mechanisms involve the dissolution of sulfur colloids, sulfur intermediates, and mineral fragments by planktonic cells (Rawlings, 2002; Tributsch, 2001). It must be highlighted that all the mechanisms involved in the bioleaching process are sustainable presenting low resources consumption and without toxic subproducts generation (He et al., 2010; Jafari et al., 2019).

In the literature, the bioleaching process have been carried out by using pure and mixed cultures. However, from an industrial biotechnology point of view, mixed culture possesses specific advantages including no sterilization requirements, the adaptive capacity due to microbial diversity, the capacity to transform different kind of wastes and the possibility of implementing continuous processes (Fernández-Morales et al., 2010; Kleerebezem and van Loosdrecht, 2007).

The mixed microbial culture growing in acid mine drainage (AMD) is characterized by the presence of acidophilic bacteria, being the most representative species *Acidithiobacillus thiooxidans, Acidithiobacillus ferrooxidans, Leptospirillum ferrooxidans and Leptospirillum ferriphilum* (Borja et al., 2019). The ADM is generated when sulfide-bearing material is exposed to oxygen and water (Akcil and Koldas, 2006). This mining effluent is characterized by its low pH, high concentration of sulfates and toxic metals (Anawar, 2013), depending its final composition on the mineral ore characteristics and on the microbial culture performing the mineral oxidation (Borja et al., 2019).

In order to achieve an efficient bioleaching process, there are several operational parameters that must be taken into account. These operational parameters could be related to the microbial metabolisms or to the transport phenomena. On the one hand, regarding to the microbial metabolisms, it is known that they are conditioned by the operational temperature, pH, redox potential and trace minerals concentrations. In the literature, it has been described that acidophilic cultures operate under mesophilic, 20° - 30° C, and thermophilic, above 45 ° C, conditions (Deng et al., 2017; Ngoma et al., 2018). Regarding to the operational pH values, it is advisable to keep a low pH below 2.0 to avoid iron precipitation and additional sludge formation (Demir et al., 2020). The redox potential is also a very important operational parameter that can also be used to identify whether the processes taking place are chemically or biologically catalyzed. The bacteria metabolisms are also controlled by the nutrients availability. In the case of the bioleaching cultures, the chemosynthetic acidophilic bacteria use ferrous iron as their main source of energy but also a wide number of trace minerals. In some cases, the metabolisms could be limited by toxicity events. In the bioleaching experiments, the presence of very high concentrations of metals, amongst other chemical species, could cause inhibition events. These inhibition

events could be minimized by a progressive adaptation of the microorganisms culture through successive sub-cultures in the presence of the inhibitory chemicals (Do Nascimento et al., 2019; Guo et al., 2013). On the other hand, regarding to the transport phenomena, the kinetics of the bioleaching processes could be enhanced by increasing the mixing and also by increasing the external surface. A higher external surface favors the contact between the microbial culture and the mineral ore, which facilitates the mass transport of the microorganisms and the chemical species involved in the bioleaching process (Ospina et al., 2011). The bioleaching process can also be enhanced by increasing the number of cells in the microbial culture. This is because the microbial concentration acts as catalysts of the process and, when operated under low microorganisms concentrations, could act as the controlling stage of the process.

In this context, the aim of this work was to develop an autochthonous acidogenic mixed culture and to study the bioleaching process of mine tailing wastes, modelling the whole bioleaching process and identifying the individual contributions. The main novelty of the study is the isolated analysis of the different contributions and the quantification of the direct as well as the indirect and cooperative mechanism’s reaction rates.

2. MATERIAL AND METHODS

2.1 Microbial inoculum and mine tailings

The initial microbial inoculum, as well as the mine tailings used in this work, were taken from real AMD of the abandoned San Quintin mine site. The San Quintín mining site is located in Ciudad Real, Spain, and it was mainly focused on the lead, zinc and silver obtention, being sphalerite (ZnS) and galena (PbS) the most significant ore minerals extracted (Rodríguez et al., 2022). The mine tailings samples were collected in disposable bags and subsequently dried at room ambient temperature for 72 hours. Then, the mine tailing samples were homogenized with 2 mm mesh and then kept in hermetic bags. Before the experiments the soil samples were grinded in an ultracentrifuge grind ZM 200. Subsequently, the solids were sieved according to the Standard ASTM D6913/D6913M-17 to obtain a particle size of 45 µm.

The first exploitation of the San Quintín mining site data from 1559, although the intensive exploitation began in 1606, being the mining closure on 1934. In 1973, the increasing prices of the metals originated a re-foundation of the mining activities, and a new froth flotation plant was installed for re-working of approximately three million tons of mineral from the tailings (Martín-Crespo et al., 2015). At present, the San Quintín mining site remains abandoned, and the ruins of the mine structures, together with mine tailings and other mining wastes resulting from the mine exploitation can be clearly recognized. These mining wastes generates environmental problems due to the transport of solid and liquid pollutants which causes, soil, as well as underground and superficial water bodies pollution, such as in the brook “Arroyo de la Mina”, which crosses this mining area.

2.2 Chemical characterization of samples

Mine tailings samples pH were measured in a 1:5 soil-water (w:v) mixture using the ISO 10390-2005 method (ISO 10390, 1994) . Electrical Conductivity (EC) was measured in a 1:5 soil-water (w:v) using a conductometer InLab 751-4mm (Mettler-Toledo, Columbus, Ohio, EEUU). Before the metal concentrations determination, samples were digested in a microwave oven (CEM MARS 5, Matthews, USA) following the procedure described in the literature, EPA 3051A method (Link et al., 1998). To do that, 0.5 g of mine tailings sample were digested with a mixture of 9 mL of 69% w:w nitric acid and 3 mL of 37% w:w hydrochloric acid. The heating conditions consists of reaching a temperature of 175ºC in 5.5 minutes, maintaining that temperature for 4.5 minutes, as required by the EPA-3051A method. The extract obtained was filtered using 110 mm Whatman^{TM} glass-fiber filter paper and the filtrate was used for subsequent analysis.

The metal concentration in the liquid samples were characterized by using an inductively coupled plasma optical emission spectrometer (ICP–OES; Varian Vista-Pro, Mulgrave, VIC, Australia). Lead (Pb), Zinc (Zn), Cadmium (Cd), Copper (Cu) and Iron (Fe) were analyzed according to the procedure described in the literature (Ilieva et al., 2018). In order to ensure the reproducibility of the tests, all the samples were analyzed in triplicate.

The results obtained during the mine tailings characterization are presented in Table 1. The mine tailing sampling point was, in the Universal Transverse Mercator coordinate system, 30S 0389247 UTM 4297326.

Table 1. Mine tailings characterization (standard deviation in brackets).

Pb	Zn	Cu	Cd	Fe	pH	Conductivity

µg/g_{dw}	µg/g_{dw}	µg/g_{dw}	µg/g_{dw}	µg/g_{dw}		µS/cm
2597 ± (74)	687 ± (15)	71.0 ± (3.8)	10.4 ± (0.2)	12902.4 ± (26)	4,76 ± (0.15)	180 ± (7.2)

2.3 Development of a steady-state acidophilic mixed culture

The inoculum taken from the AMD of the San Quintin mining site was growth in 250 ml Erlenmeyer flasks fed with 100 ml of the TK medium as growth media. The TK solution was obtained by mixing two solutions A and B. Solution A, contained in (g/L) $(NH_4)_2SO_4$ (0.625), $MgSO_4.7H_2O$ (0.625) and KH_2PO_4 (0.625), the pH of this solution was adjusted to 2.0 with a 1 mol/L H_2SO_4 solution and then sterilized at 121 °C for 20 min; Solution B only contained the $FeSO_4.7H_2O$ required as energy source for the growth and activity of the acidogenic microorganisms, its pH was adjusted to 2.0 by using a 1 mol/L H_2SO_4 solution. In order to sterilize the solution B, a sterilizing filtration through s a 0.2 µm pore size membrane was carried out according to the literature (Utimura et al., 2019). The growth medium was prepared by mixing 650 mL of solution A, with 250 mL of solution B and with 100 ml of deionized waster to reach a final volume of 1L.

In order to obtain a steady-state microbial culture, the inoculum taken from San Quintin mining site was grown on 150 mmol Fe^{2+}/L in the TK medium by sequential batches during 50 d. At the end of this stage, an autochthonous steady-state mixed acidophilic culture was obtained. This process was employed to obtain a significant amount of mixed culture of acidophilic bacteria able to oxidize ferrous iron without experiencing lag phases or inhibitory events (Utimura et al., 2019).

The performance of every cycle was mathematically modelled and only once the most sensitive parameter, the maximum ferrous iron oxidation rate, was constant the culture was supposed to be under steady state conditions. With the aim to extend the kinetic and

stoichiometric characterization of the steady-state culture developed, the effect of the initial ferrous iron concentration was studied. To do that, the steady-state culture was subjected to different initial ferrous-iron concentrations ranging from 150 to 50 mmol Fe^{2+}/L.

2.4 Bioleaching Experiments

Once obtained the autochthonous steady-state culture, it was used in the mine tailings biolixiviation experiments carried out. With the aim to study the different mechanisms taking place in the biolixiviation process, a series of experiments were carried out at different pulp densities 1, 5, 10 and 20 % w/v. Bioleaching Experiments were carried out in 250 ml Erlenmeyer flasks in an orbital incubator (MaxQ 4000, Thermo Scientific, Waltham, Massachusetts, EEUU) at 150 rpm agitation speed, at 303 K and containing 100 ml of TK medium. The inoculum used was the steady-state acidophilic mixed culture previously developed during the grown of the mixed microbial population contained in the AMD of the San Quintín mining site. 1 ml of mixed culture was used as seed in each flask for bioleaching test. The bioleaching progress and microbial activity was on-line monitored by measuring redox potential and pH. The redox potential was determined by using a RedOx probe (HI 98120, Hanna Instruments, Woonsocket, Rhode Island, EEUU) the pH was determined by using a pH probe (HI-1131B, Hanna Instruments, Woonsocket, Rhode Island, EEUU). Additionally, discrete measurements of other parameters such as: acid and alkali consumption, ferrous and ferric-iron concentrations as well as total concentrations of Fe, Pb, Zn, Cu, and Cd were carried out.

Parallel to the series of bioleaching experiments, abiotic tests were carried out. These tests were identical to the bioleaching experiments, being the only difference the absence of

microbial inoculum. These abiotic tests were used to isolate the chemical reactions taking place in the system when no microbial activity took place. Comparing the biotic and the abiotic experiments the main biological processes can be isolated.

2.5 Mathematical model

The different bioleaching experiments were mathematically modelled, and the main process parameters were determined with the aim to evaluate the performance of the microbial population obtained in each subculture. The model used was based on that previously proposed in the literature (Breed and Hansford, 1999a) (Boon et al., 1999) and widely used (Abbasi et al., 2021).

In this model, it has been proposed that the ferrous-iron oxidation can be described by a function depending on the ferric to ferrous-iron ratio.

$$-r_{Fe^{2+}} = q_{Fe^{2+}} \cdot C_x \qquad \text{[Eq. 7]}$$

$$q_{Fe^{2+}} = \frac{q_{Fe^{2+}}^{max}}{1 + K_{Fe^{2+}} \frac{Fe^{3+}}{Fe^{2+}}} \qquad \text{[Eq. 8]}$$

$$-r_{Fe^{2+}} = r_{Fe^{3+}} = \frac{1}{Y_{s/x}^{max}} \cdot r_x + m_s \cdot C_x \qquad \text{[Eq. 9]}$$

Where $q_{Fe^{2+}}$ is the specific ferrous-iron oxidation rate, C_x is the biomass concentration, $q_{Fe^{2+}}^{max}$ is the maximum specific ferrous-iron oxidation rate, $K_{Fe^{2+}}$ is the apparent affinity constant, $Y_{s/x}^{max}$ is the maximum biomass yield and m_s is the maintenance coefficient.

In order to fit the model to the experimental results, the set of equations of the model was solved simultaneously using the Gauss-Newton algorithm. An initial set of values was

assigned to the model parameters and, after several iterations, the values of the parameters that minimised of the sum of squared errors (SSE) were chosen as the best estimate (de Lucas et al., 2007). The SSE expression used to estimate the value of the model parameters was:

$$\chi\ (p) = \frac{\sqrt{\sum_{i=1}^{n}\left(z_{meas,i} - z_i(p)\right)^2}}{\overline{z}} + \frac{\sqrt{\sum_{i=1}^{n}\left(y_{meas,i} - y_i(p)\right)^2}}{\overline{y}} + \frac{\sqrt{\sum_{i=1}^{n}\left(x_{meas,i} - x_i(p)\right)^2}}{\overline{x}} \quad \text{[Eq. 10]}$$

Where x, y and z are the model variables ferrous, ferric-iron and biomass concentration respectively, $x_{meas,I,}$ $y_{meas,i}$ and $z_{meas,i}$ are the ith measurement of the ferrous-iron, ferric-iron and biomass concentrations, $x_i(p)$, $y_i(p)$ and $z_i(p)$ are the calculated values of the model variables corresponding to the ith measurement. $\overline{x}$, $\overline{y}$ and $\overline{z}$ are the mean between the maximum and minimum value of the measurements and *n* is the number of data points.

3. RESULTS

3.1. Steady-state microbial culture

With the aim to obtain a steady-state microbial culture from the raw AMD taken at the San Quintin mining site, the original seed was subjected to several batch subcultures in which the ferrous-iron oxidation was studied. In these cycles, the microorganisms were exposed to a TK medium containing 150 mmol/L of ferrous-iron. Figure 1 presents the ferrous-iron profile during the first culture as well as the abiotic reference test carried out.

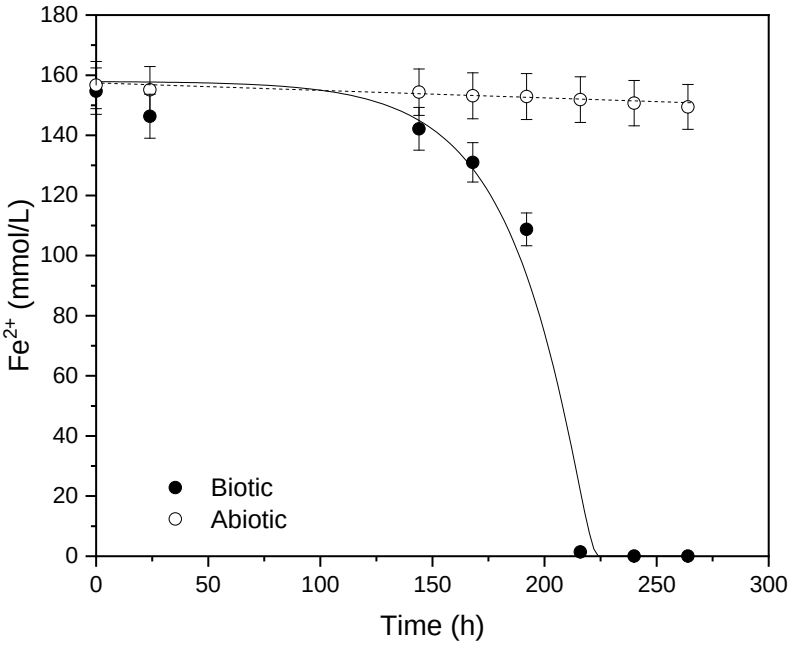

Figure 1. Ferrous-iron oxidation during the first acclimatization batch culture. Conditions: pH 2.0, 303 K and 150 rpm.

As can be seen in Figure 1, the ferrous-iron oxidation in the abiotic test was negligible, even after 12 d. However, an insignificant ferrous iron oxidation took place due to the acidic conditions and the presence of oxygen. These reactions caused a slight change in

color of the bulk solution, this slight color change could be associated to the production of colloidal ferrous hydroxide sulphate generated by the abiotic reactions presented in Eq. 5-6.

$$4FeSO_4 + O_2 + 2H_2SO_4 \rightarrow 4Fe(OH)(SO_4) \quad \text{[Eq. 5]}$$

$$4FeSO_4 + O_2 + (2-n)H_2SO_4 \rightarrow Fe_2(OH)_n(SO_4)_{3-n/2} + (2-2n)H_2O \quad \text{[Eq. 6]}$$

In the first culture of the biotic tests, it was observed a lag phase of about 4 d. Then, the ferrous-iron oxidation started, being necessary 10 d to obtain the complete oxidation of the 150 mmol Fe^{2+}/L. The full-grown microbial culture, with only logarithmic phase bacteria, was then subcultured several times. As the microbial culture was subcultured, the microbial population was adapted to the media and the biomass concentration increased, reducing the length of the lag phase to a negligible value and increasing the maximum ferrous-iron oxidation rate. The different subcultures results were mathematically modelled using the model previously proposed. This model used was based on that proposed in the literature (Breed and Hansford, 1999a) (Boon et al., 1999) and widely used (Abbasi et al., 2021). From the modelling works, the kinetic and stoichiometric coefficients of the model were determined. In Figure 2 it can be seen the evolution of the $q_{Fe^{2+}}^{max}$, the most sensitive parameter of the model, obtained in the successive subculturing.

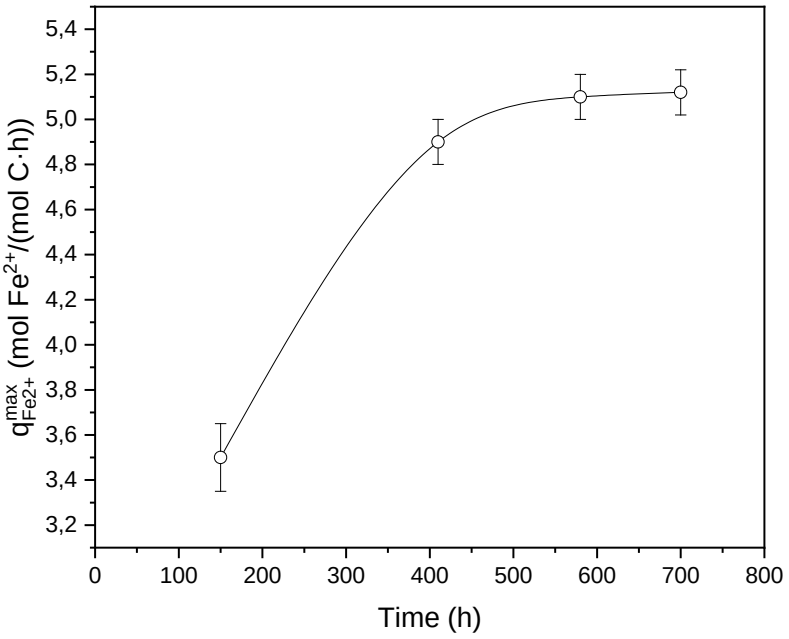

Figure 2. Maximum ferrous iron oxidation rates along the acclimatization period. Conditions: pH 2.0, 303 K and 150 rpm.

As can be seen in Figure 2, the value of the $q_{Fe^{2+}}^{max}$ increased up to the 4th time of subculturing, in which a constant value was observed in the ferrous-iron oxidation rate. During the subsequent sub-culturing, after 29 d of acclimatization, the value of the $q_{Fe^{2+}}^{max}$ remained constant at about 5.1 (mmol Fe^{2+}/(mmol C·h)), the $K_{Fe^{2+}}$ at 0.005 and the $Y_{s/x}^{max}$ at 0.001 mmol C/ mmol Fe^{2+}. Because of the steady-state values reached, the mixed population culture was supposed to be under steady-state conditions.

In the literature, the microbial population of similar AMD cultures have been characterized observing that the most frequent microbial population were *Acidithiobacillus ferroxidans* and *Leptospirillum ferroxidans* (Edwards et al., 2000, 1999; Méndez-García et al., 2015). The *Leptospirillum spp* have been described to be predominant in environments with high

redox potentials, about 800 mV, and high acidic conditions, pH below 1.5 (Coram and Rawlings, 2002) such as in the inoculum took from the AMD ponds almost completely oxidated of the San Quintin Mining site. This can be explained because *Leptosipirllum* strains presents a higher affinity for ferrous-iron than *Acidithiobacillus ferroxidans* (apparent K_m 0.25 mM Fe^{2+} versus 1.34 mM for *Acidithiobacillus ferroxidans*) and a lower affinity for ferric-iron, which according to the literature is a competitive inhibitor (Coram and Rawlings, 2002; Rawlings et al., 1999).

Taking into account this information, and the characteristics of the AMD from where the initial inoculum was taken, it is suggested that the microbial culture mainly contained a combined population of *Acidithiobacillus ferroxidans* and *Leptospirillum* strains. From the comparison of the steady-state values obtained in the modelling works for the $q_{Fe^{2+}}^{max}$ and the $K_{Fe^{2+}}$ with the values described in the literature (Ebrahimi et al., 2005), it seems that the most relevant population was the *Leptospirillum* strains which, according to the literature, was characterised by a $q_{Fe^{2+}}^{max}$, a $K_{Fe^{2+}}$and a $Y_{s/x}^{max}$ of 6.8 mmol Fe^{2+}/(mmol C·h), 0.005 and 0.01 mmol C/mmol Fe^{2+} respectively, values very similar to those obtained in the steady-state mixed microbial culture of this study. These findings were ratified by means of matrix-assisted laser desorption/ionization time-of-flight mass spectroscopy (MALDI-TOF MS).

3.2. Study of the Fe^{2+} oxidation

The microbial ferrous-iron oxidation kinetics must be well studied before studying a bioleaching process since it is a critical sub-process in the bioleaching of the sulphides minerals ore (Ojumu et al., 2009). The main roles of the ferrous-iron are its participation in the indirect and cooperative bioleaching process, as well as the key role of the ferrous-iron

on the biomass growth of the microbial culture performing the direct bioleaching process. In the literature it has been studied the ferrous-iron oxidation by mixed microbial cultures. Unfortunately, most studies were performed at a fixed total iron concentration, being in most of the cases 10 g/L, 185 mmol Fe^{2+}/L (Petersen and Ojumu, 2007). Recently, the application of heap bioleaching for mining wastes, where total iron concentrations are usually less than 100 mmol/L of ferrous-iron requires a wider study of the effect of the total iron concentration (Coram and Rawlings, 2002; Petersen and Ojumu, 2007). Because of that, with the aim to study the effect of ferrous-iron concentration lower than 185 mmol Fe^{2+}/L, three batch tests were performed operating at different initial ferrous-iron concentrations. The concentrations studied were 150, 100 and 50 mmol/L of ferrous-iron. The main results obtained during the ferrous-iron bioxidation tests as well as the modelling results when operating at the different initial ferrous-iron concentrations are presented in Figure 3. The ferrous-iron oxidation in the blank tests were negligible and the results are not presented in the figures for the sake of clarity.

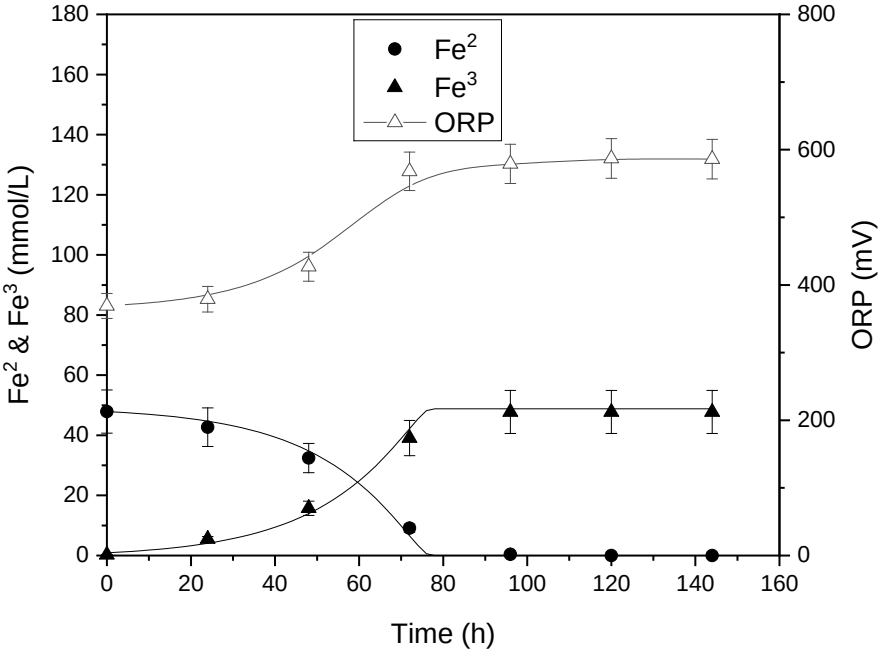

a)

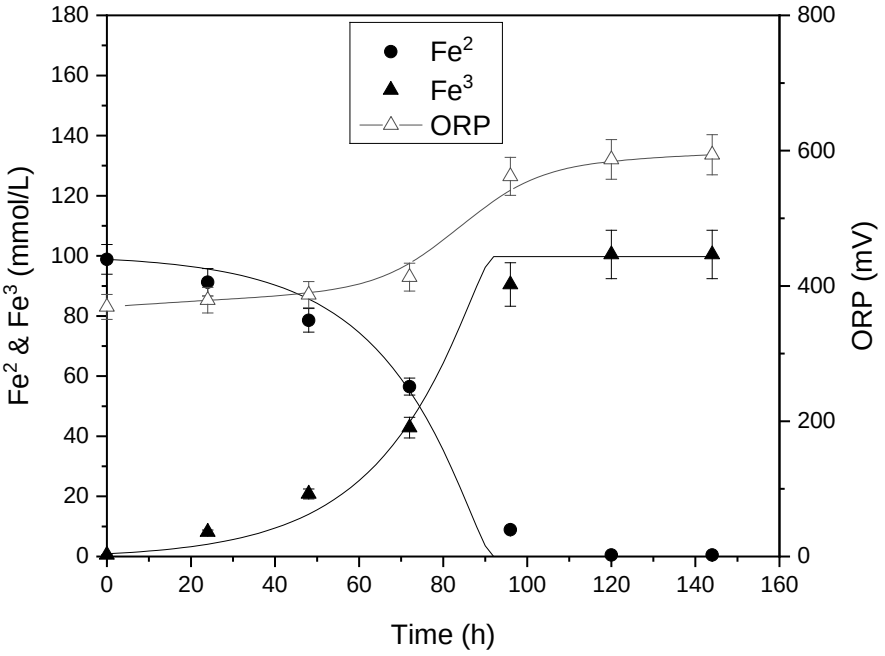
Fe2
Fe3
ORP
Fe2 & Fe3 (mmol/L)
ORP (mV)
Time (h)
0
20
40
60
80
100
120
140
160
180
200
400
600
800

b)

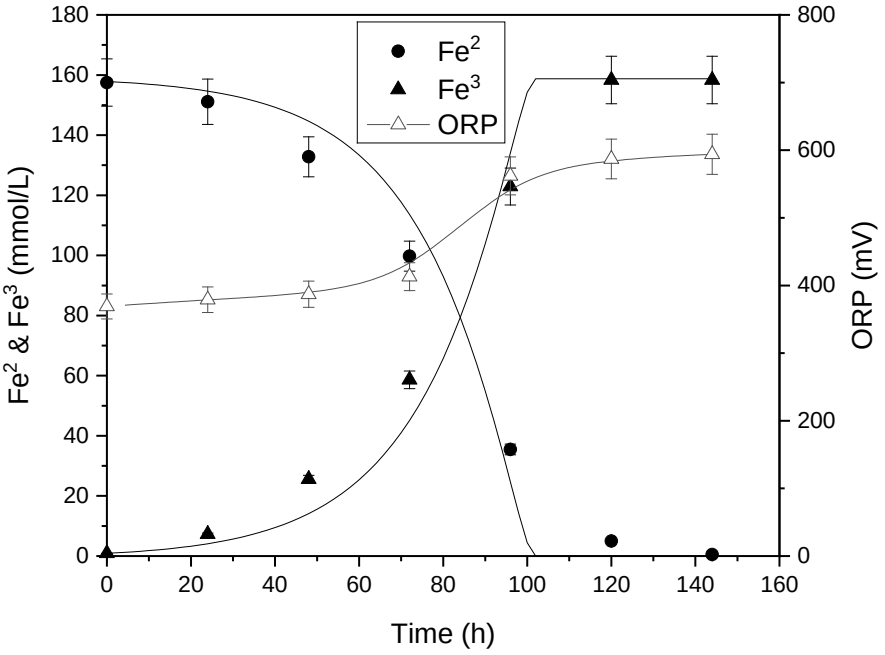
Fe2
Fe3
ORP
Fe2 & Fe3 (mmol/L)
ORP (mV)
Time (h)
0
20
40
60
80
100
120
140
160
180
200
400
600
800

c)

Figure 3. Ferrous-iron, redox potential and biomass concentration along the tests carried out at different ferrous-iron concentrations. a) 50 mmol/L, b) 100 mmol/L and c) 150 mmol/L Conditions: pH 2.0, 303 K and 150 rpm. Lines indicate model fit.

In order to characterize the performance of the iron oxidizing process when operating at the three different initial ferrous-iron concentrations, the model previously proposed in Eqs. 7-9 was fitted to the experimental results obtained. From the modelling works, accurate predictions of the process behavior were obtained as can be seen in Figure 3. The parameter values obtained from the modelling works were those presented in Table 2. As can be seen in this table, the $q_{Fe^{2+}}^{max}$ and the $K_{Fe^{2+}}$ presented the values of the steady-state culture, 5.1 mmol Fe^{2+}/(mmol C·h) and 0.005, being this value independent of the initial ferrous-iron concentration, within the range of concentrations used in this study. This result indicated that no mass transfer limitations occur when decreasing the ferrous-iron concentration from 150 to 50 mmol Fe^{2+}/L. The maximum biomass yield on ferrous-iron decreased from 0.0100 to 0.0092 mmol C/mmol Fe^{2+}, when the ferrous-iron was increased from 50 to 150 mmol Fe^{2+}/L. Analogous biomass yields have been described in the literature when operating under similar conditions (Breed et al., 1999; Breed and Hansford, 1999b; Ojumu et al., 2009; Ojumu and Petersen, 2011; van Scherpenzeel et al., 1998). Regarding with the maximum biomass growth rate, its value decreased from 0.040 to 0.033 h^{-1}, when the ferrous iron increased from 50 to 150 mmol Fe^{2+}/L. This behavior could be explained by an increase in the maintenance requirements when increasing the ferrous-iron concentration. A similar observation has been described in the literature when operating with *Leptospirillum* strains (van Scherpenzeel et al., 1998). The value obtained for the μ_{max}, 0.04 h^{-1}, was very similar to that presented in the literature for the range of ferrous-iron concentration and

operational conditions of this study (Nemati and Harrison, 2000). Once determined the value of the μ_{max}, the doubling time (td) was determined as the quotient between Ln 2 and μ_{max}. The results obtained for the μ_{max} and the td are presented in Table 2. Similar results of the μ_{max} and td have been described in the literature (Ojumu et al., 2009; Ojumu and Petersen, 2011).

Table 2. Parameters values estimation from the modelling of the ferrous-iron oxidation process.

		Ferrous-iron concentration (mmol/L)		
Parameter	**Unit**	**150**	**100**	**50**
$q_{Fe^{2+}}^{max}$	mmol Fe^{2+}/(mmol C ·h)	5.1	5.1	5.1
$K_{Fe^{2+}}$		0.005	0.005	0.005
$Y_{s/x}^{max}$	mmol C/mmol Fe^{2+}	0.0092	0.0095	0.0100
μ_{max}	h^{-1}	0.0332	0.0390	0.0400
td	h	20.88	17.74	17.30

Additionally, with the aim to ratify the values obtained for the main operational parameters in the mathematical fitting of the model, the maximum specific iron oxidation rate as well as the apparent affinity constant were determined by means of the Lineweaver-Burk representation. To do that, the equation describing the ferrous-iron evolution, presented in Eq. 8, was linearized and $q_{Fe^{2+}}$ was represented vs the ratio Fe^{3+}/Fe^{2+}. As can be seen in Figure 4, it was possible to fit simultaneously the data corresponding to the three different initial ferrous-iron concentrations studied in this work with a very high correlation coefficient, 0.997. This result indicates that no significant differences were observed when changing the initial ferrous-iron within the range studied in this work, 50-150 mmol Fe^{+2}/L.

From the intercept of the representation the $q_{Fe^{2+}}^{max}$ was determined, 5.0 mmol Fe^{2+}/(mmol C·h), being its value very similar to that obtained from the mathematical modelling based on the minimization of the SSE, 5.1 mmol Fe^{2+}/(mmol C·h).

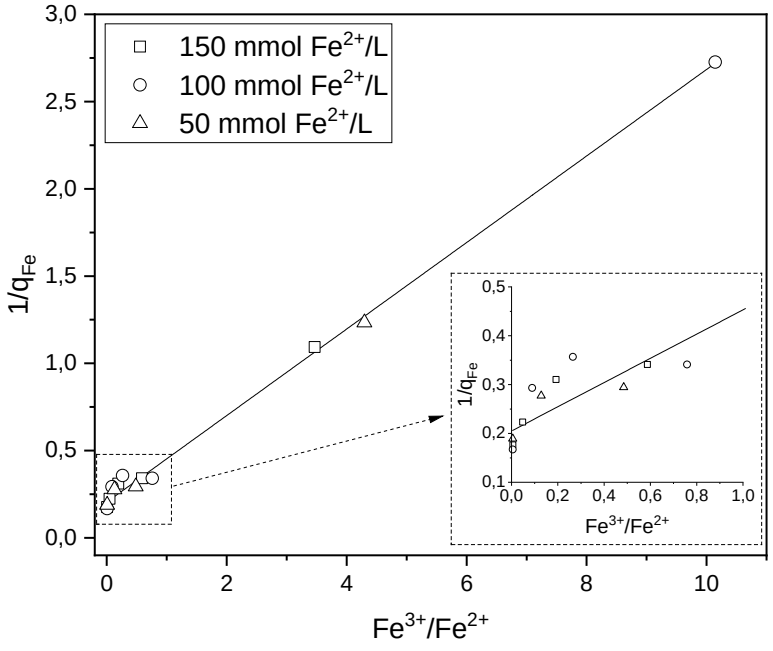

Figure 4. Lineweaver-Burk representation of the data obtained at the different initial ferrous-iron concentrations.

From the slope of the representation the $K_{Fe^{2+}}$ was determined. In this case, the $K_{Fe^{2+}}$ value obtained from the Lineweaver-Burk representation, 1.23, was significantly different to that obtained from the mathematical modelling based on the minimization of the SSE, 0.005. This difference can be explained because most of the data point were located at low Fe^{3+}/Fe^{2+} ratios, being the number of data corresponding to high ratios scarce, which significantly affect the fitting value of the slope. The difference in the $K_{Fe^{2+}}$ value could be

also explained because the $K_{Fe^{2+}}$ is not a sensitive parameter in the model conditions used in this work.

3.3. Mine tailing lixiviation

Once obtained a steady-state mixed microbial culture and characterized its ability to oxidize ferrous-iron, the biolixiviation process of the mine tailings was studied. Parallel, abiotic tests were performed at the different pulp densities, ranging from 1, 5, 10 and 20 % w/v, were studied. In the abiotic test it was observed a negligible metal dissolution. This can be explained because, on the one hand, the mine tailings studied were previously stored under environmental conditions during decades at the abandoned San Quintin mining site, reacting and lixiviating the easily soluble fractions and, on the other hand, the lack of microorganisms does not allow the catalyzed solubilization. Similar results have been described in the literature (Nagar et al., 2021).

In the biotic tests carried out with the mine tailings, it was observed an increasing metal dissolution when increasing the pulp density, see Figure 5a. However, the specific metal dissolved presented a maximum value when operated at the minimum pulp density, 1% w/v, as can be seen in Figure 5b. Similar results have been described in the literature (Cazón et al., 2014; Venkatesa Prabhu et al., 2019). This behavior can be explained taking into account that the amount of inoculum was the same in all the cases. Under these circumstances, the biomass concentration could act as the limiting stage of the metal dissolution when operating at high pulp densities. In other words, the increase in the pulp density does not increase the metal dissolution due to the limited microbial culture available. Moreover, high pulp densities could facilitate the biofilm detachment due to the erosion caused by the higher frictions taking place when operating at very high pulp

densities. This detachment would affect to the direct lixiviation mechanism and therefore to the metal dissolution. The metal recovery when performing the biolixiviation at a 1% pulp density was about 90% of Cd, 60% of Zn, 30% of Cu and 6% of Pb. The low lead recovery could be explained because these mine tailings were reprocessed for lead extraction, remaining only the less available lead and because of the metal speciation remaining in the mine tailings used in this study (Ge et al., 2022).

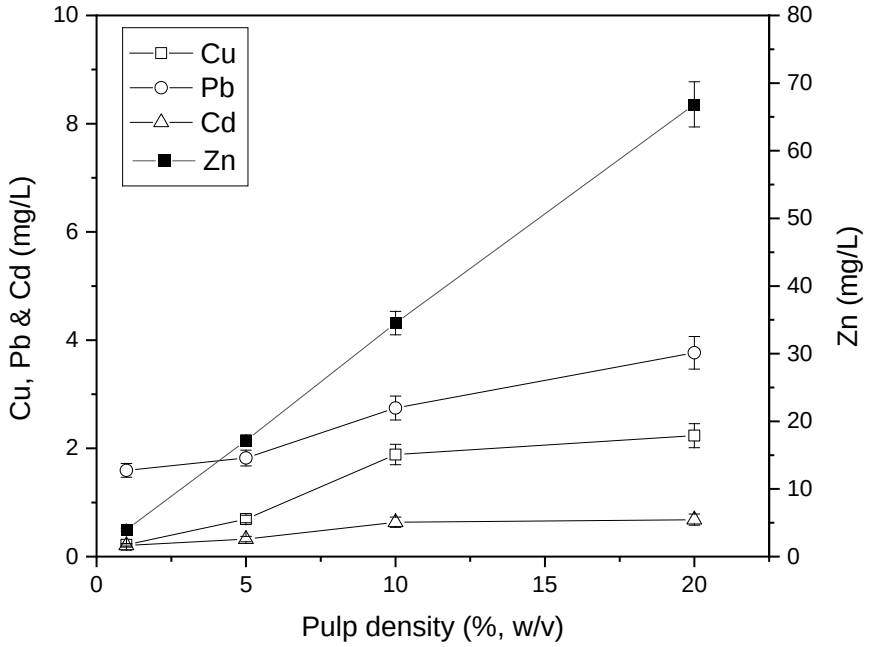

a)

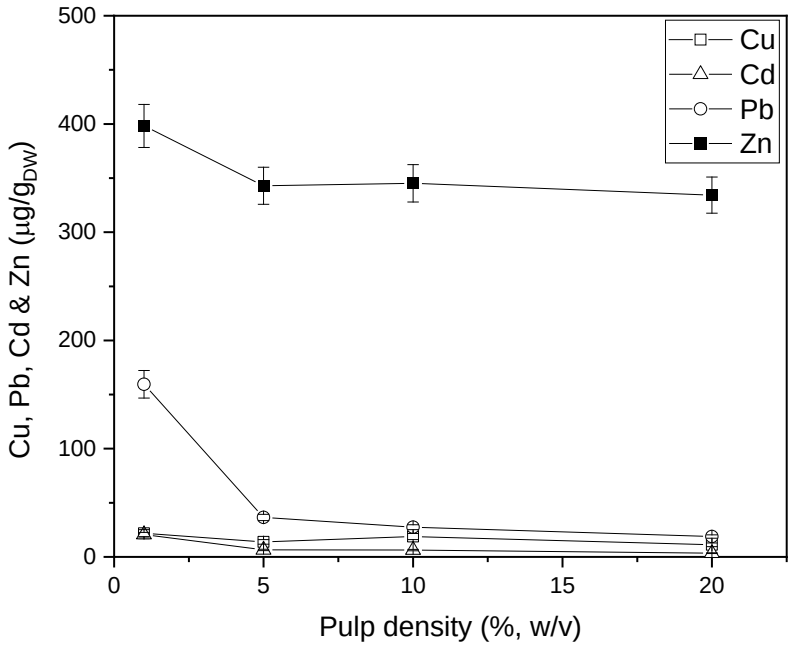

b)

Figure 5. a) Absolute metal dissolved at the end of the bioleaching experiments and b) specific metal dissolved at the end of the bioleaching experiments.

Analyzing the iron dissolved from the mineral ore during the bioleaching process of the mine tailings, results presented in Figure 6a, it was observed a non-proportional increase of the total iron dissolution when increasing the pulp density. Moreover, it can be observed a lag phase when operating at pulp densities of 5, 10 and 20 % w/v. With the aim to analyze the process behavior, the specific total iron dissolution was also calculated, and the result obtained are presented in Figure 6b.

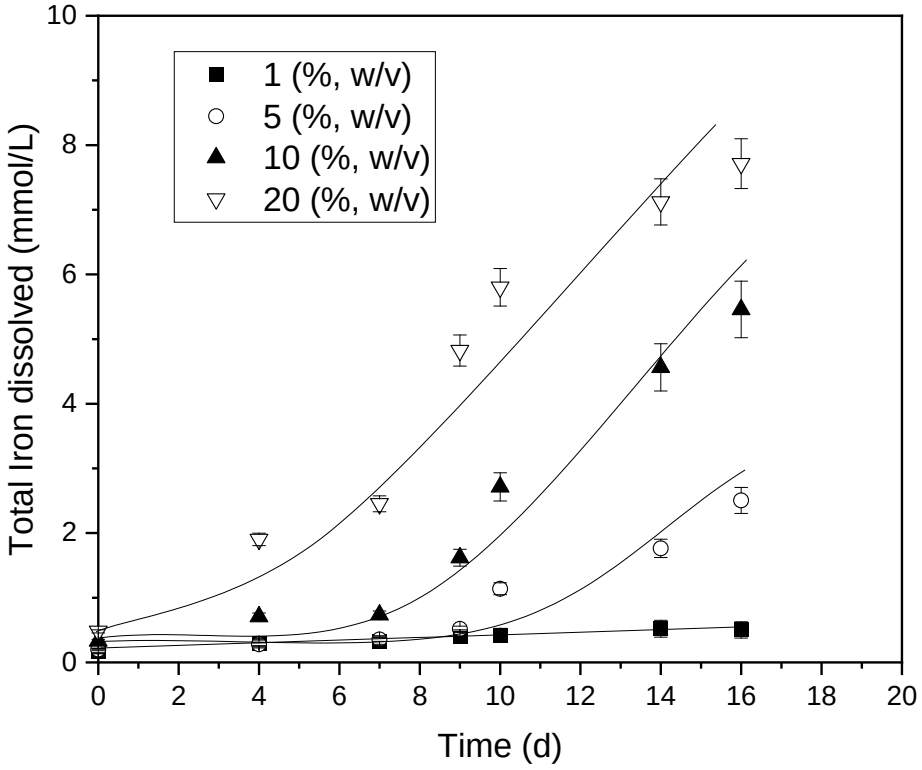
1 (%, w/v)
5 (%, w/v)
10 (%, w/v)
20 (%, w/v)
Total Iron dissolved (mmol/L)
Time (d)
0
2
4
6
8
10
12
14
16
18
20

a)

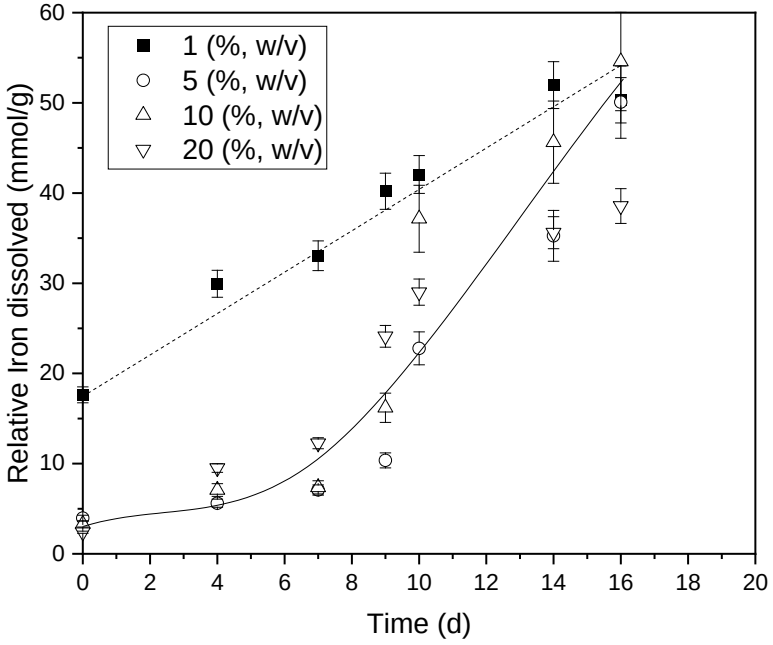
1 (%, w/v)
5 (%, w/v)
10 (%, w/v)
20 (%, w/v)
Relative Iron dissolved (mmol/g)
Time (d)
0
10
20
30
40
50
60
0
2
4
6
8
10
12
14
16
18
20

b)

Figure 6. a) Absolute total iron dissolution along the bioleaching experiments and b) specific total iron dissolution along the bioleaching experiments.

From the specific total iron dissolution, Figure 6 b, it can be observed that, when operating at the lowest pulp density, 1% w/v, no lag phase took place in the bioleaching process. However, when operating at higher pulp densities a lag phase was observed in all the cases indicating that a limitation took place in the process. This limitation could be related to the lack of biomass, which could act as the limiting reactant in the biolixiviation process when operating at high pulp densities, being necessary to develop a higher biomass concentration to increase the specific biolixiviation rate. These results ratify the results presented for the other metals, Cd, Cu, Zn and Pb, where the maximum relative metal dissolution was also obtained when operating at the lowest pulp density, 1% w/v.

With the aim to deep into the knowledge of the metal lixiviation of the mine tailings and to identify the contribution of the different mechanism during the metal dissolution, the ferrous and ferric-iron evolution along the biolixiviation process were modelled. In the literature, it has been described that the lixiviation process can be described by means of three different mechanisms: direct, indirect and cooperative mechanisms (Figueroa-Estrada et al., 2020; Sajjad et al., 2019). The model used in this work was based on the main reactions taking place in these mechanisms.

The direct mechanism is related to the direct electron transference from the mineral to the microorganism that are in contact with the ore, resulting the mineral dissolution due to the electrochemical processes taking place. This mechanism requires the presence of attached microorganisms able to directly exchange the electron with the mineral ore. The main reactions taking place in this mechanism are the ferrous-iron dissolution and the

subsequently microbial oxidation of the ferrous to ferric-iron, see Eq. 11 and 1 respectively (Belzile et al., 2004).

$$2\,FeS_2 + 7\,O_2 + 2\,H_2O \xrightarrow{Bacteria} 2\,Fe^{2+} + 4\,SO_4^{2-} + 4\,H^+ \qquad \text{[Eq. 11]}$$

The solubilization of the ferrous-iron was modelled by using the kinetic equation proposed on Eq. 12. Once solubilized the ferrous-iron, it was oxidized to generate ferric-iron. Based on the model previously described in Eqs. 7-9, the kinetics of this oxidation process was modelled by using the eq. 13.

$$\frac{dFe^{2+}}{dt} = K_d \cdot Cx \cdot Pd \qquad \text{[Eq. 12]}$$

$$\frac{dFe^{3+}}{dt} = -\frac{dFe^{2+}}{dt} = \frac{q_{Fe^{2+}}^{max}}{1 + K_{Fe^{2+}}\frac{Fe^{3+}}{Fe^{2+}}} \cdot Cx \qquad \text{[Eq. 13]}$$

Where K_d is the direct reaction rate, and Pd is the pulp density.

The indirect mechanism is caused by the ferric-iron present in the liquid bulk. In acidic conditions, the ferric-iron acts as an oxidizing and lixiviating agent that dissolve the ferrous-iron contained in the ore. Because of that, ferrous-iron is released from the ore at the same time that the lixiviating ferric-iron is reduced to ferrous-iron. The chemical reaction taking place in the indirect mechanisms is presented in Eq. 14.

$$FeS + Fe_2(SO_4)_3 \xrightarrow{Chemical} FeSO_4 + 2FeSO_4 + S^0 \qquad \text{[Eq. 14]}$$

The indirect bioleaching mechanisms is a chemically controlled reaction in which the ferric-iron acts as the limiting reagent when it is in excess of ore. This is a pure chemical

process, and its kinetics was described in this work by using a first order equation according to the literature (McKibben and Barnes, 1986).

$$\frac{dFe^{2+}}{dt} = -\frac{dFe^{3+}}{dt} = K_i \cdot \frac{[Fe^{3+}]^{0.5}}{[H^+]^{0.5}} \qquad \text{[Eq. 15]}$$

Where K_i is the indirect mechanism reaction rate.

Anyway, the microorganisms are indirectly involved because its key role on the reoxidation of the ferrous to ferric-iron and on the acid generation according to Eqs. 1-2.

Finally, the cooperative bioleaching refers to the mineral dissolution caused by sulfur intermediates, sulfur colloids, planktonic microorganisms, etc. (Rawlings, 2002). These mechanisms describe, in a holistic way, several mechanisms that synchronously dissolve the mineral (Figueroa-Estrada et al., 2020; Sajjad et al., 2019). This mechanism was described by a first order kinetics function of the pulp density. Although it is difficult to conceptualize this mechanism in a theoretical basis, the dissolution phenomena of a solid particle in a liquid media implies a surface action that depends on the pulp density. Because of that, and based on the Noyes–Whitney Equation for solute dissolution (Hattori et al., 2013) the following first order kinetics was proposed in this work:

$$\frac{dFe^{2+}}{dt} = K_c \cdot Pd \qquad \text{[Eq. 16]}$$

where K_c is the cooperative mechanism reaction rate.

The set of equations proposed for the bioleaching mechanisms was simultaneously fitted to the experimental results obtained with all the pulp densities studied by minimizing the SSE

as previously described. From the fitting of the model to the data series a very good fitting was obtained. In Figure 7 it is presented the experimental data as well as the modelling results obtained when operating with a pulp density of 20% w/v.

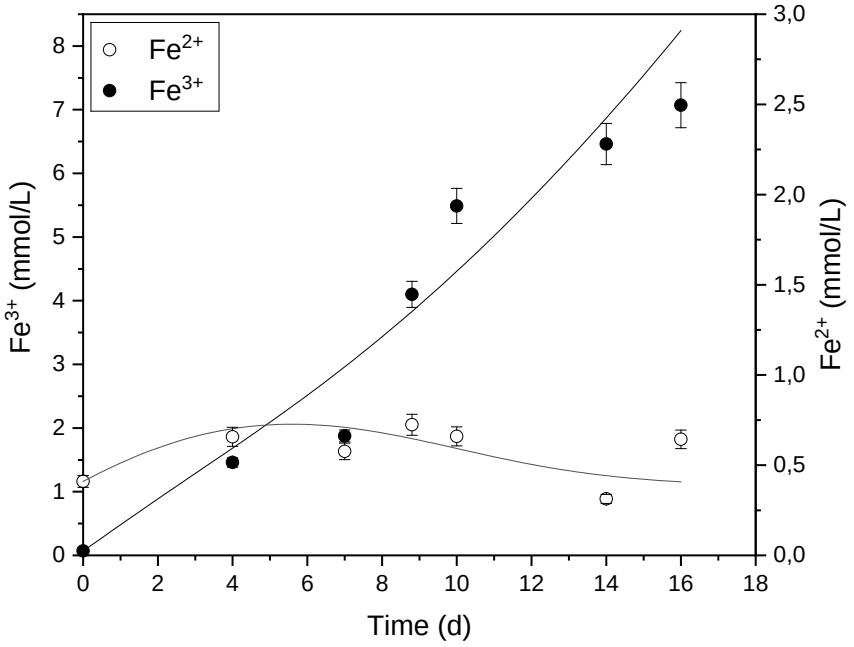

a)

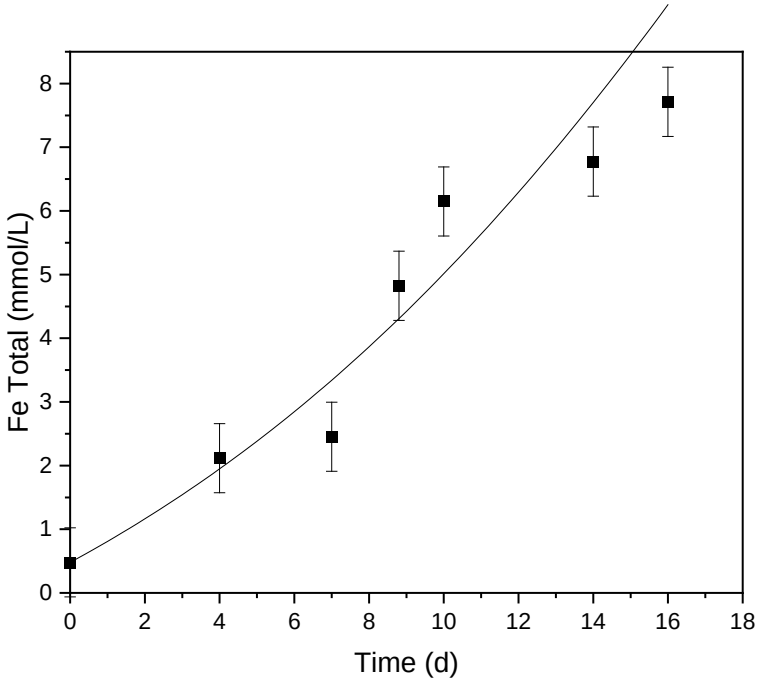

b)

Figure 7. Experimental results, (data points) and modelling results, lines, of the bioleaching of iron from mine tailings at a 20% w/v pulp density. a) Ferrous and ferric iron b) Total iron.

The values of the model parameters describing the different mechanisms are presented in Table 3. As can be seen in this table, all the model parameter were fitted with the same values except the maximum ferrous-iron oxidation rate. This can be explained because the lower the the pulp density the lower the ferrous-iron concentration in the liquid bulk, which led to an increasing the mass transfer limitations. Additionally, the value of the ferrous iron oxidation was significantly lower to that obtained when oxidizing ferrous iron concentrations within 50-150 mmol Fe^{2+}/L, which can also be explained in terms of the mass transfer limitations experienced when operating at all the pulp densities studied. From

this modelling it was obtained that, in the case of the pyrite, the direct mechanisms account for a 85% of the ferrous-iron dissolution and the indirect and cooperative mechanisms account for a 15% being not possible to identify the individual contributions of the indirect and cooperative rates because of the lack of identifiability and sensitivity of the model equations describing these mechanisms (Brun et al., 2001).

Table 3. Parameters values estimation from the modelling of the bioleaching of the mine tailings.

		Pulp density (% w/v)			
Parameter		**1**	**5**	**10**	**20**
$q_{Fe^{2+}}^{max}$	mmol Fe^{2+}/(mmol C ·h)	0.015	0.085	0.20	0.35
$K_{Fe^{2+}}$		0.005	0.005	0.005	0.005
K_d	mmol Fe^{2+}/(mmol C·% w/v·h)	0.017	0.017	0.017	0.017
K_i	mmol Fe^{2+}·(mol H^+)$^{0.5}$/((mol Fe^{3+})$^{0.5}$·(h))	0.002	0.002	0.002	0.002
K_c	mmol Fe^{2+}/(% w/v·h)	0.001	0.001	0.001	0.001

CONCLUSIONS

Based on the results obtained in this work, it can be concluded that the autochthonous culture was able to extract most of the Cd, Fe and Zn contained in the mine tailings. The ferrous-iron oxidation by the autochthonous culture was studied and modelled obtaining a maximum ferrous-iron oxidation of 5.1 mmol Fe^{2+}/(mmol C·h) and a biomass yield of 0.01 mmol C/ mmol Fe^{2+}, values very similar to those presented by the *Leptosipirrillum* strains. From the bioleaching experiment of the mine tailings, it was observed that the experiment

with 1% w/v pulp density exhibit the highest efficiency of leaching as 90% of Cd, 70% Fe, 60% of Zn, 30% of Cu and 6% of Pb were extracted. When the bioleaching pulp density increased, the efficiency decreased because of the biomass concentration acts as the limiting stage of the biolixiviation mechanisms, thus reducing the leaching ability of the process. Finally, the pyrite lixiviation mechanisms were studied obtaining the rates of the direct, indirect and cooperative mechanisms, observing that about 85% of the ferrous-iron dissolution corresponds to the direct mechanisms and 15% to the indirect and cooperative mechanisms.

Acknowledgements

Financial support from the following sources is gratefully acknowledged: Project SBPLY/19/180501/000254 from European Union (FEDER) and Castilla-La Mancha regional government, and Projects PID2019-107282RB-I00 and EQC2018-004240-P from Ministry of Science, Innovation and Universities.

References

Abbasi, M., Aminian-Dehkordi, J., Mousavi, S.M., 2021. A novel computational simulation approach to study biofilm significance in a packed-bed biooxidation reactor. Chemosphere 262. https://doi.org/10.1016/j.chemosphere.2020.127680

Akcil, A., Koldas, S., 2006. Acid Mine Drainage (AMD): causes, treatment and case studies. J Clean Prod. https://doi.org/10.1016/j.jclepro.2004.09.006

Anawar, H.M., 2013. Impact of climate change on acid mine drainage generation and contaminant transport in water ecosystems of semi-arid and arid mining areas. Physics and Chemistry of the Earth 58–60, 13–21. https://doi.org/10.1016/j.pce.2013.04.002

Azapagic, A., 2004. Developing a framework for sustainable development indicators for the mining and minerals industry, in: Journal of Cleaner Production. Elsevier, pp. 639–662. https://doi.org/10.1016/S0959-6526(03)00075-1

Belzile, N., Chen, Y.W., Cai, M.F., Li, Y., 2004. A review on pyrrhotite oxidation. J Geochem Explor 84. https://doi.org/10.1016/j.gexplo.2004.03.003

Boon, M., Ras, C., Heijnen, J.J., 1999. The ferrous iron oxidation kinetics of Thiobacillus ferrooxidans in batch cultures. Appl Microbiol Biotechnol 51. https://doi.org/10.1007/s002530051467

Borja, D., Nguyen, K.A., Silva, R.A., Ngoma, E., Petersen, J., Harrison, S.T.L., Park, J.H., Kim, H., 2019. Continuous bioleaching of arsenopyrite from mine tailings using an adapted mesophilic microbial culture. Hydrometallurgy 187. https://doi.org/10.1016/j.hydromet.2019.05.022

Breed, A.W., Dempers, C.J.N., Searby, G.E., Gardner, M.N., Rawlings, D.E., Hansford, G.S., 1999. The effect of temperature on the continuous ferrous-iron oxidation kinetics of a predominantly Leptospirillum ferrooxidans culture. Biotechnol Bioeng 65. https://doi.org/10.1002/(SICI)1097-0290(19991005)65:1<44::AID-BIT6>3.0.CO;2-V

Breed, A.W., Hansford, G.S., 1999a. Studies on the mechanism and kinetics of bioleaching. Miner Eng 12. https://doi.org/10.1016/S0892-6875(99)00018-7

Breed, A.W., Hansford, G.S., 1999b. Effect of pH on ferrous-iron oxidation kinetics of Leptospirillum ferrooxidans in continuous culture. Biochem Eng J 3. https://doi.org/10.1016/S1369-703X(99)00018-2

Brun, R., Reichert, P., Künsch, H.R., 2001. Practical identifiability analysis of large environmental simulation models. Water Resour Res 37. https://doi.org/10.1029/2000WR900350

Cazón, J.P., Yagnentovsky, N., Viera, M., Donati, E., 2014. Application of integrated microbial processes for heavy metal recovery from industrial wastes of Buenos Aires, Argentina, in: Bioremediation in Latin America: Current Research and Perspectives. https://doi.org/10.1007/978-3-319-05738-5_9

Ciftci, H., Atik, S., 2017. Microbial leaching of metals from a lateritic nickel ore by pure and mixed cultures of mesophilic acidophiles. Metallurgical Research and Technology 114. https://doi.org/10.1051/metal/2017049

Coram, N.J., Rawlings, D.E., 2002. Molecular relationship between two groups of the genus Leptospirillum and the finding that Leptospirillum ferriphilum sp. nov. Dominates south African commercial biooxidation tanks that operate at 40°C. Appl Environ Microbiol 68. https://doi.org/10.1128/AEM.68.2.838-845.2002

de Lucas, A., Rodríguez, L., Villaseñor, J., Fernández, F.J., 2007. Fermentation of agro-food wastewaters by activated sludge. Water Res 41. https://doi.org/10.1016/j.watres.2007.01.041

Delgado, Y., Fernández-Morales, F.J., Llanos, J., 2021. An old technique with a promising future: Recent advances in the use of electrodeposition for metal recovery. Molecules. https://doi.org/10.3390/molecules26185525

Demir, E.K., Yaman, B.N., Çelik, P.A., Sahinkaya, E., 2020. Iron oxidation in a ceramic membrane bioreactor using acidophilic bacteria isolated from an acid mine drainage. Journal of Water Process Engineering 38, 101610. https://doi.org/10.1016/j.jwpe.2020.101610

Deng, S., Gu, G., Wu, Z., Xu, X., 2017. Bioleaching of arsenopyrite by mixed cultures of iron-oxidizing and sulfur-oxidizing microorganisms. Chemosphere 185, 403–411. https://doi.org/10.1016/j.chemosphere.2017.07.037

Deveci, H., Akcil, A., Alp, I., 2004. Bioleaching of complex zinc sulphides using mesophilic and thermophilic bacteria: Comparative importance of pH and iron. Hydrometallurgy 73, 293–303. https://doi.org/10.1016/j.hydromet.2003.12.001

Do Nascimento, D.N.O., Lucheta, A.R., Palmieri, M.C., Do Carmo, A.L.V., Silva, P.M.P., Ferreira, R.V. de P., Junca, E., Grillo, F.F., Alves, J.O., 2019. Bioleaching for copper extraction of marginal ores from the Brazilian Amazon region. Metals (Basel) 9, 1–13. https://doi.org/10.3390/met9010081

Ebrahimi, S., Fernández Morales, F.J., Kleerebezem, R., Heijnen, J.J., van Loosdrecht, M.C.M., 2005. High-rate acidophilic ferrous iron oxidation in a biofilm airlift reactor and the role of the carrier material. Biotechnol Bioeng 90. https://doi.org/10.1002/bit.20448

Edwards, K.J., Bond, P.L., Gihring, T.M., Banfield, J.F., 2000. An Archaeal iron-oxidizing extreme acidophile important in acid mine drainage. Science (1979) 287. https://doi.org/10.1126/science.287.5459.1796

Edwards, K.J., Gihring, T.M., Banfield, J.F., 1999. Seasonal variations in microbial populations and environmental conditions in an extreme acid mine drainage environment. Appl Environ Microbiol 65. https://doi.org/10.1128/aem.65.8.3627-3632.1999

Fernández-Morales, F.J., Villaseñor, J., Infantes, D., 2010. Modeling and monitoring of the acclimatization of conventional activated sludge to a biohydrogen producing culture by biokinetic control. Int J Hydrogen Energy 35. https://doi.org/10.1016/j.ijhydene.2010.07.054

Figueroa-Estrada, J.C., Aguilar-López, R., Rodríguez-Vázquez, R., Neria-González, M.I., 2020. Bioleaching for the extraction of metals from sulfide ores using a new chemolithoautotrophic bacterium. Hydrometallurgy 197. https://doi.org/10.1016/j.hydromet.2020.105445

Ge, D., Huang, S., Cheng, J., Han, Y., Wang, Y., Dong, Y., Hu, J., Li, G., Yuan, H., Zhu, N., 2022. A new environment-friendly polyferric sulfate-catalyzed ozonation process for sludge conditioning to achieve deep dewatering and simultaneous detoxification. J Clean Prod 359, 132049. https://doi.org/10.1016/J.JCLEPRO.2022.132049

Ghorbani, M., Nowee, S.M., Ramezanian, N., Raji, F., 2016. A new nanostructured material amino functionalized mesoporous silica synthesized via co-condensation method for Pb(II) and Ni(II) ion sorption from aqueous solution. Hydrometallurgy 161, 117–126. https://doi.org/10.1016/j.hydromet.2016.02.002

Guo, Y.G., Huang, P., Zhang, W.G., Yuan, X.W., Fan, F.X., Wang, H.L., Liu, J.S., Wang, Z.H., 2013. Leaching of heavy metals from Dexing copper mine tailings pond. Transactions of Nonferrous Metals Society of China (English Edition) 23, 3068–3075. https://doi.org/10.1016/S1003-6326(13)62835-6

Hattori, Y., Haruna, Y., Otsuka, M., 2013. Dissolution process analysis using model-free Noyes-Whitney integral equation. Colloids Surf B Biointerfaces 102. https://doi.org/10.1016/j.colsurfb.2012.08.017

He, Z., Shengmu, A.E., Ae, X., Ae, X.X., Hu, Y., 2007. Microbial diversity in acid mineral bioleaching systems of dongxiang copper mine and Yinshan lead-zinc mine. https://doi.org/10.1007/s00792-007-0130-x

He, Z., Zhao, J., Gao, F., Hu, Y., Qiu, G., 2010. Monitoring bacterial community shifts in bioleaching of Ni-Cu sulfide. Bioresour Technol 101, 8287–8293. https://doi.org/10.1016/j.biortech.2010.05.047

Holden, W.N., 2015. Mining amid typhoons: Large-scale mining and typhoon vulnerability in the Philippines. Extractive Industries and Society 2. https://doi.org/10.1016/j.exis.2015.04.009

Huang, T., Li, D., 2014. Presentation on mechanisms and applications of chalcopyrite and pyrite bioleaching in biohydrometallurgy - A presentation. Biotechnology Reports. https://doi.org/10.1016/j.btre.2014.09.003

Ilieva, D., Surleva, A., Murariu, M., Drochioiu, G., Abdullah, M.M.A.B., 2018. Evaluation of ICP-OES method for heavy metal and metalloids determination in sterile dump material, in: Solid State Phenomena. https://doi.org/10.4028/www.scientific.net/SSP.273.159

ISO 10390, 1994. Soil Quality - Determination of pH. International standard 3.

Jafari, M., Abdollahi, H., Shafaei, S.Z., Gharabaghi, M., Jafari, H., Akcil, A., Panda, S., 2019. Acidophilic bioleaching: A Review on the Process and Effect of Organic–inorganic Reagents and Materials on its Efficiency. Mineral Processing and Extractive Metallurgy Review 40, 87–107. https://doi.org/10.1080/08827508.2018.1481063

Kleerebezem, R., van Loosdrecht, M.C., 2007. Mixed culture biotechnology for bioenergy production. Curr Opin Biotechnol. https://doi.org/10.1016/j.copbio.2007.05.001

Link, D.D., Walter, P.J., Kingston, H.M., 1998. Development and validation of the new EPA microwave-assisted leach method 3051A. Environ Sci Technol 32. https://doi.org/10.1021/es980559n

Martín-Crespo, T., Gómez-Ortiz, D., Martín-Velázquez, S., Esbrí, J.M., de Ignacio-San José, C., Sánchez-García, M.J., Montoya-Montes, I., Martín-González, F., 2015. Abandoned mine tailings in cultural itineraries: Don Quixote Route (Spain). Eng Geol 197. https://doi.org/10.1016/j.enggeo.2015.08.008

McKibben, M.A., Barnes, H.L., 1986. Oxidation of pyrite in low temperature acidic solutions: Rate laws and surface textures. Geochim Cosmochim Acta 50. https://doi.org/10.1016/0016-7037(86)90325-X

Méndez-García, C., Peláez, A.I., Mesa, V., Sánchez, J., Golyshina, O. v., Ferrer, M., 2015. Microbial diversity and metabolic networks in acid mine drainage habitats. Front Microbiol. https://doi.org/10.3389/fmicb.2015.00475

Nagar, N., Garg, H., Sharma, N., Awe, S.A., Gahan, C.S., 2021. Effect of pulp density on the bioleaching of metals from petroleum refinery spent catalyst. 3 Biotech 11. https://doi.org/10.1007/s13205-021-02686-y

Nemati, M., Harrison, S.T.L., 2000. Comparative study on thermophilic and mesophilic biooxidation of ferrous iron. Miner Eng 13. https://doi.org/10.1016/S0892-6875(99)00146-6

Ngoma, E., Borja, D., Smart, M., Shaik, K., Kim, H., Petersen, J., Harrison, S.T.L., 2018. Bioleaching of arsenopyrite from Janggun mine tailings (South Korea) using an adapted mixed mesophilic culture. Hydrometallurgy 181, 21–28. https://doi.org/10.1016/j.hydromet.2018.08.010

Nguyen, K.A., Borja, D., You, J., Hong, G., Jung, H., Kim, H., 2018. Chalcopyrite bioleaching using adapted mesophilic microorganisms: Effects of temperature, pulp density, and initial ferrous concentrations. Mater Trans 59, 1860–1866. https://doi.org/10.2320/matertrans.M2018247

Ojumu, T. v., Hansford, G.S., Petersen, J., 2009. The kinetics of ferrous-iron oxidation by Leptospirillum ferriphilum in continuous culture: The effect of temperature. Biochem Eng J 46. https://doi.org/10.1016/j.bej.2009.05.001

Ojumu, T. v., Petersen, J., 2011. The kinetics of ferrous ion oxidation by Leptospirillum ferriphilum in continuous culture: The effect of pH. Hydrometallurgy 106. https://doi.org/10.1016/j.hydromet.2010.11.007

Ospina, J., Restrepo, E.M., Osorno Bedoya, L., Antonio Márquez, M., Morales, A.L., 2011. Biooxidation of arsenopyrite concentrates by Acidithiobacillus ferrooxidans in shake flasks, Rev. Colomb. Biotecnol.

Petersen, J., Ojumu, T.V., 2007. The Effect of Total Iron Concentration and Iron Speciation on the Rate of Ferrous Iron Oxidation Kinetics of *Leptospirillum ferriphilum* in Continuous Tank Systems. Adv Mat Res 20–21. https://doi.org/10.4028/www.scientific.net/amr.20-21.447

Rawlings, D.E., 2002. Heavy metal mining using microbes. Annu Rev Microbiol. https://doi.org/10.1146/annurev.micro.56.012302.161052

Rawlings, D.E., Tributsch, H., Hansford, G.S., 1999. Reasons why 'Leptospirillum'-like species rather than Thiobacillus ferrooxidans are the dominant iron-oxidizing bacteria in many commercial processes for the biooxidation of pyrite and related ores. Microbiology (N Y). https://doi.org/10.1099/13500872-145-1-5

Rodríguez, L., González-Corrochano, B., Medina-Díaz, H.L., López-Bellido, F.J., Fernández-Morales, F.J., Alonso-Azcárate, J., 2022. Does environmental risk really change in abandoned mining areas in the medium term when no control measures are taken? Chemosphere 291. https://doi.org/10.1016/j.chemosphere.2021.133129

Sajjad, W., Zheng, G., Din, G., Ma, X., Rafiq, M., Xu, W., 2019. Metals Extraction from Sulfide Ores with Microorganisms: The Bioleaching Technology and Recent Developments. Transactions of the Indian Institute of Metals. https://doi.org/10.1007/s12666-018-1516-4

Tributsch, H., 2001. Direct versus indirect bioleaching. Hydrometallurgy 59. https://doi.org/10.1016/S0304-386X(00)00181-X

Utimura, S.K., Arevalo, S.J., Rosario, C.G.A., Aguilar, M.Q., Tenório, J.A.S., Espinosa, D.C.R., 2019. Bioleaching of metal from waste stream using a native strain of Acidithiobacillus isolated from a coal mine drainage. Canadian Journal of Chemical Engineering 97. https://doi.org/10.1002/cjce.23519

van Scherpenzeel, D.A., Boon, M., Ras, C., Hansford, G.S., Heijnen, J.J., 1998. Kinetics of ferrous iron oxidation by Leptospirillum bacteria in continuous cultures. Biotechnol Prog 14. https://doi.org/10.1021/bp980016h

Venkatesa Prabhu, S., Baskar, R., Ramesh, G., Adugna, A.T., 2019. Bioleaching of zinc and iron from sphalerite using leptospirillum ferriphilum: Kinetic aspects. International Journal of Scientific and Technology Research 8.